Decision and control system for a solar powered train

Beatriz Féria
Instituto Superior Técnico/Institute for Systems and Robotics
maria.stoffel@ist.utl.pt
João Sequeira
Instituto Superior Técnico/Institute for Systems and Robotics
joao.silva.sequeiral@ist.utl.pt

***Abstract*—This paper addresses the design and simulation of a control system for a solar powered train. An intelligent control approach is followed aiming at managing the energy consumption such that the train always reaches its destination, never risking a shortage of energy. The whole infrastructure is modeled as a discrete event system, using Petri nets, for which a supervisory controller is designed.**

The energy management system handles all energy consumption devices onboard the train, namely, solar panels, batteries, sensors and computational devices, in order to ensure that the train finishes its mission successfully. The system uses a priori information on the topology of the line, e.g., length and slopes, locations of the intermediate stations, dynamics of the train, current solar irradiance and weather forecasting, and passenger weight to determine bounds on the train velocity profile.

The whole system was simulated integrating Petri nets in a Matlab/Simulink environment. A discussion on several results obtained is presented in the paper.

Keywords: *Solar powered train, Petri nets, Supervisory control, Energy management system*

I. INTRODUCTION

This paper describes ongoing work under the framework of project Helianto aiming at designing a light solar powered train for the transportation of tourists along beach shores.

The Helianto solar train is an autonomous vehicle, powered exclusively by solar energy and batteries. This makes it an economical, emissions free and attractive mean of transportation, namely for touristic purposes, that can be used to establish the connection between urban centers and environmentally sensitive areas, e.g., beach shores, where no electric power supply lines can be installed. The train is equipped with an array of solar panels that can adjust their orientation in order to maximize the solar energy captured. A set of batteries is also installed onboard being recharged, through the electric grid, whenever the train is stopped at a station and using energy regenerated from braking.

In general energy consumption can be reduced by using light materials, and tailored aerodynamics. The Helianto velocities range does not exceed values around 30km/h, due to limited power supply, and hence the role of aerodynamics can be neglected. However, trains moving on steel rails use their own weight to improve traction and hence reducing it below a certain level may not be an option. Though adding important weight, batteries still have low energy density and hence the long recharging times. Thus, their use needs to be carefully managed, so that when the solar power is not enough they can provide enough energy for the train to complete the journey. These are precisely the kind of factors that can be tested with the simulation environment developed in order to optimize (i) the design of the train subsystems, and (ii) the design of the operation procedures.

Figure 1 shows an artistic impression of the Helianto solar powered train for touristic purposes.

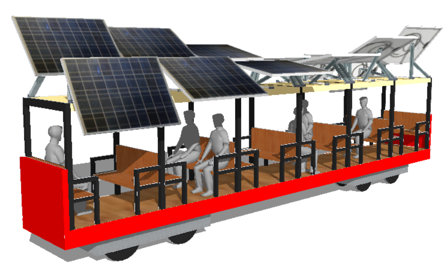

Figure 1. An artistic view of the Helianto ultralight solar train.

There have been several approaches to the implementation of control systems for vehicles running on limited energy sources and energy management systems have been extensively studied in a multitude of applications [1], [2]. The ultimate goal of energy management systems is to achieve maximum average efficiency depending on the vehicles' performance purpose (high speed, high autonomy etc). The average efficiency has to take into account several external conditions such as route gradient and surface, predicted meteorological conditions and also the forces opposing the motion, gravity, rolling resistance and aerodynamic drag [1]. In order to study and develop the energy management system, all the components dealing with energy onboard the train and even those located in the outside, namely at the stations and along the railway line have to be modeled realistically. In the Helianto project, the overall system is modeled through discrete events systems (DES) [3] specifically Petri Nets. Modeling the overall system through discrete event systems allows the supervisory energy management system to account for all relevant events. DES and the design of supervisory controllers [4] has been extensively described in the literature such as in [9] and [10]. Moreover, DES have an elegant representation in the form of Petri nets, for which there are available powerful analysis tools [5] and for which supervisory controller design techniques allow an easy inclusion of constraints found in this type of application.

This paper is organized as follows. Section II discusses the infrastructure for a solar power train, together with some of the modeling options and tools used for the simulation in section III. In fact, the paper described just an example of a possible infrastructure for the whole system, from train to the stations. Section IV presents a Petri net model of the overall system, with the corresponding supervisory controller being described in section V. Simulation results are discussed in Section VI, and the conclusions of the paper are presented in Section VII.

II. Basis Infrastructure

A key assumption of the project is that the topology of the line and the placement of the stations placed along the line are known. The train uses GPS and the information on the topology of the line, eventually with a selection of landmarks placed along the line, for pinpoint positioning accuracy. Obstacle detection sensors, e.g., laser range finders.

Each station is equipped with a gate through which the passengers must go through to access train. The gate system keeps count on how many people are in the station. Moreover, weight sensors at the gate floor allow an estimate the total weight to board the train at each station.

The energy management system uses information from all energy sources and sinks and also from environmental conditions. For example, an internet connection is used to access short term weather forecast services for the region where the train is operating, if available.

The relevant events are defined after (i) the desired operation conditions, and (ii) any contingency situations and constraints. Among the key ones are, (i) low irradiance, preventing the panels from delivering power, (ii) obstacles in the line, (iii) loss of satellite signal, (iv) weather and weight changes, and (v) communications failure, for example when receiving weather forecast or any other necessary variable.

Given an a priori defined time schedule for the train, specifying the arrival and departure times at each station, the goal of the supervisory controller is defined as generate a velocity profile reference such that (i) the train complies with the schedule, even in presence of unexpected events, (ii) the use of energy from the battery set is minimized, and (iii) the velocity and acceleration are always within operational limits defined by passenger comfort.

Figure 2 presents the block diagram designed for the global controlled system.

The supervisory controller receives information from the solar panels, obstacles detection laser, and weight sensors. Along with the information from the location tracking block, the supervisor defines an admissible cruise velocity and communicates the reference to the low level velocity control block. In case the velocity allowed by the energy generated by the solar panels is below the minimum required for the train to comply with the mission parameters, the system resorts to the batteries.

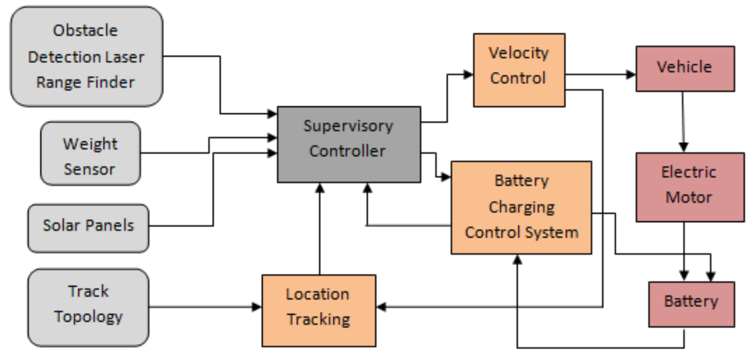

Figure 2. Block diagram of the overall system.

The location tracking block uses information from the track topology. Along with the feedback from the velocity estimate, it computes in real-time the estimate of the train position so that an adequate braking time is computed and the vehicle stops at the stations. The estimate for the train position can be computed using standard fusion techniques. Since it is a low-speed train, skid is discarded and thus the dead-reckoning estimate can be fused with GPS using the standard Kalman filtering technique to get an accurate estimate.

Once a reference velocity is defined by the velocity control block, the vehicle block communicates to the motor block the necessary torque which in turn generates the necessary power.

The battery charging control block is responsible for keeping the battery charge within a certain range. In case the battery reaches the minimum charge value, the block prevents further discharging and signals the system that the battery needs to be charged at the next station. A safe charge value to be provided at each station in order to ensure the train arrives at the next station in case of low irradiance, obstacles in the way or even communication failure, is also defined.

III. Simulation Environment

A simulation tool was developed under Simulink environment with the purpose of assessing feasibility studies concerning solar vehicle projects. It consists in a practical and flexible tool that allows the simulation of multiple types of vehicles, multiple track features, different energy sources as well as different performance purposes for the vehicle. Two key toolboxes were used, QSS [12] and Netlab [11]. The combined use of these toolboxes results in a powerful simulation environment which even allows hardware-in-the-loop testing.

A. Netlab

Netlab is the tool used to design the Petri net model. It consists in a Windows interface that allows the design and graphical simulation of Petri Nets. This tool also interfaces Matlab/Simulink allowing Simulink to import the Petri nets created in Netlab as a single block. In combination with Simulink, the Petri nets can be extended with input and output places. When a place is set as an input, its marking is determined by Simulink and if it is set as an output its marking is transferred to Simulink. Therefore, the exchange of data between the Petri net and the rest of the environment is reduced to the marking in input and output places.

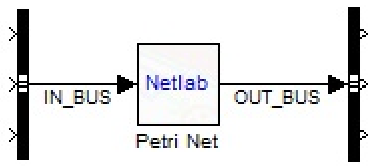

(a) Petri Net block under Simulink environment.

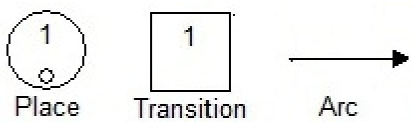

(b) Petri Net model symbols.

Figure 3. Element symbols from Netlab environment.

Figure 3(a) illustrates the Petri net block in Simulink and the input and output buses that establish communication between signals from Simulink and the Petri net. Figure 3(b) illustrates the Netlab Petri net element symbols used to design the Petri net model. Supervisory control is then applied to the overall system through the Petri net block, establishing a direct, real-time, communication with Simulink.

B. QSS

The QSS toolbox permits a flexible design of powertrain systems and a fast estimation of the energy consumption of such systems. The low computational power required makes the QSS an interesting computational platform to model and simulate powertrains. It consists in a discrete tool that simulates the behavior of a vehicle, motor and energy source, given a desired velocity and acceleration profile. For each step time interval a profile, that includes velocity, acceleration and track gradient is defined for the vehicle. The velocity and acceleration profile is calculated based on information from the location tracking block, panels and sensors. The track gradient profile is defined based on track topology and location tracking block. These inputs are assumed to be constant for each step time, which for the purpose of this work was set to 1 second. At each step the torque required for the vehicle to follow the specified velocity profile is calculated, together with the energy consumption necessary to sustain it. For this project, three blocks from the QSS toolbox, were used in the simulation: the vehicle, the electric motor and the battery blocks. These three blocks are shown in figure 4.

The vehicle block accounts for specifications such as overall vehicle weight, wheel diameter, frontal area and friction and

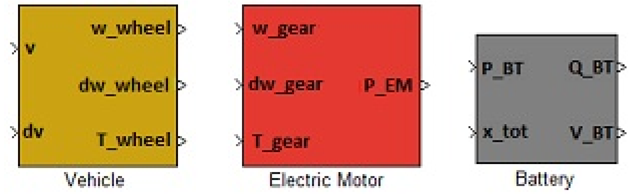

Figure 4. QSS library vehicle, electric motor, and battery blocks.

drag coefficients. It outputs the required torque measured at the wheels, rotational speed and acceleration. The torque is determined so that the vehicle meets the input velocity and acceleration and is described as the sum of aerodynamic drag force, acceleration force, rolling resistance and gravitational force.

The motor block outputs the power required by the motor in order to produce the required torque. It includes specifications such as motor inertia and scaling factor.

The battery block outputs the current charge of the battery as well as the consumption per kilometer, in case distance traveled is provided at the input. The input corresponds to the power demanded or delivered to the battery, respectively positive or negative. In this block it is necessary to specify variables such as battery capacity, initial charge and current limit.

IV. Petri Net Model

The overall Petri Net is divided into several sub-systems. Each of these sub-systems was individually designed and tested. In the final stage, all of the sub-systems are joined together in order to form the whole system. The model represents the main states of the system as well as the events triggering the transitions between them.

A. Train

Figure 5(a) shows the Petri net designed for this sub-system. Each of the main states is represented by places. A single token is passed on from place to place representing the current situation of the train. Once the train is ready, it starts movement when transition 1 is triggered, representing a start command. While moving two events can occur: a station approaches (transition 5) or the laser detects an obstacle (transition 3). The first leads the train to stop and remain on a terminal state waiting to proceed to the next trunk. The second also leads the train to stop and wait for permission to finish the current trunk.

B. Motor

Figure 5(b) represents the Petri net that models the electric motor. There are four main operation modes for the motor and each one is represented by a place: motor off, accelerating, cruise velocity, and decelerating mode. The presence of a token in one of these places indicates the current mode of the motor. Once the motor is started (transition 6) it accelerates until the vehicle reaches the referenced cruise velocity (transition 7). Once this happens the motor switches to cruise velocity

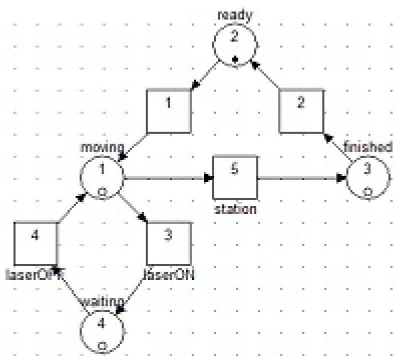

$$M_0=\begin{bmatrix} 1 & 0 & -1 & 1 & -1 \\ -1 & 1 & 0 & 0 & 0 \\ 0 & -1 & 0 & 0 & 1 \\ 0 & 0 & 1 & -1 & 0 \end{bmatrix} u_0=\begin{bmatrix} 0 \\ 1 \\ 0 \\ 0 \end{bmatrix}$$

(a) Petri net representing the train.

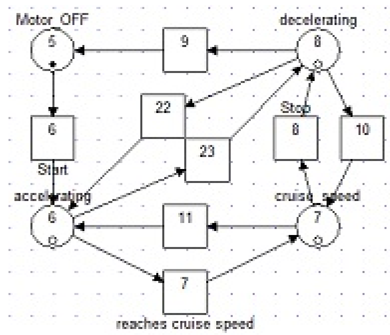

$$M_1=\begin{bmatrix} -1 & 0 & 0 & 1 & 0 & 0 & 0 & 0 \\ 1 & -1 & 0 & 0 & 0 & 1 & 1 & -1 \\ 0 & 1 & -1 & 0 & 1 & -1 & 0 & 0 \\ 0 & 0 & 1 & -1 & -1 & 0 & -1 & 1 \end{bmatrix} u_1=\begin{bmatrix} 1 \\ 0 \\ 0 \\ 0 \end{bmatrix}$$

(b) Petri net representing the motor.

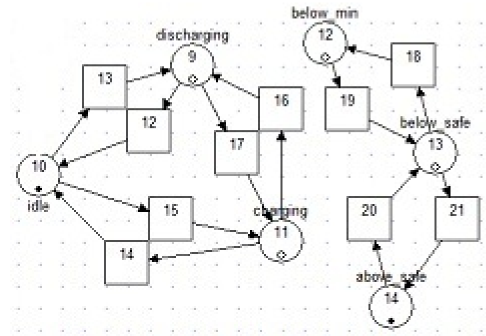

$$M_2=\begin{bmatrix} -1 & 1 & 0 & 0 & 1 & -1 & 0 & 0 & 0 & 0 \\ 1 & -1 & 1 & -1 & 0 & 0 & 0 & 0 & 0 & 0 \\ 0 & 0 & -1 & 1 & -1 & 1 & 0 & 0 & 0 & 0 \\ 0 & 0 & 0 & 0 & 0 & 0 & 1 & -1 & 0 & 0 \\ 0 & 0 & 0 & 0 & 0 & 0 & -1 & 1 & 1 & -1 \\ 0 & 0 & 0 & 0 & 0 & 0 & 0 & 0 & -1 & 1 \end{bmatrix} u_2=\begin{bmatrix} 0 \\ 1 \\ 0 \\ 0 \\ 0 \\ 1 \end{bmatrix}$$

(c) Petri net representing the battery.

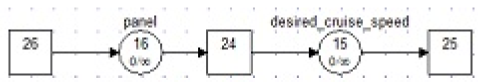

$$M_3=\begin{bmatrix} 1 & -1 & 0 \\ -1 & 0 & 1 \end{bmatrix} u_3=\begin{bmatrix} 0 \\ 0 \end{bmatrix}$$

(d) Petri net representing the desired velocity determination.

Figure 5. Petri Net model representing the various sub-systems and respective incident matrices ans initial conditions.

mode. From this mode two possible events can occur: the vehicle stops (transition 8), and in that case the motor switches to decelerating mode or the vehicle is allowed to increase cruise velocity (transition 11) and in that case it switches to accelerating mode. Transition 8 can be set by three different types of events. The first occurs when the train approaches a station, then transition 8 fires leading the motor to decelerate until it stops. The second occurs when the laser range finder detects an object. If this happens the train is required to stop and transition 8 fires leading the vehicle to decelerate until it stops. In case the obstacle is no longer detected (transition 22) it is possible for the vehicle to switch from decelerating mode to accelerating mode in order to resume previous motion. Finally transition 8 can also be set by another event, which is power decrease. If the output power of panels can no longer support current cruise velocity, transition 8 fires and the motor decelerates until a supported velocity is reached. It is also possible that this situation is reversed. This means that if the output power of panels increases, so does the supported cruise velocity and the motor switches to accelerating mode (transition 11) until it reaches the new cruise velocity.

C. Battery

The battery is modeled according to two important characteristics: the stages of operation and the battery charge level condition. Figure 5(c) shows the Petri net designed for the battery.

There are three possible stages of operation for the battery: idle, charging and discharging. If the power delivered by the panels is not enough to sustain minimum cruise velocity, the battery is allowed to discharge the necessary power so that the vehicle reaches that velocity. Also during accelerating mode, where a power peak demand occurs, the battery is allowed to discharge since the power requested during this mode is higher than the panels can support. If none of these situations occur, the battery remains in an idle stage waiting for a discharging or charging request.

The battery enters charging mode whenever the motor decelerates, through the regenerative braking system or at the stations, through the power grid, whenever the charge is below the safety value.

The battery condition is also modeled by three main states: above safety value, below safety value and below minimum value. The minimum value represents a characteristic property of each type of battery that states that the battery charge should never cross that threshold, at the risk of malfunction.

The safe value represents the necessary charge stored in the battery that ensures the train reaches the next station considering situations such as low irradiance, obstacles on the track or even communication failure. At every station this value should be ensured, by charging the battery through the power grid when necessary. If the battery charge remains between these two values the token remains in the place representing below safe state.

D. Cruise Speed Reference

The Petri net represented in figure 5(d) defines the desired cruise speed for the vehicle directly from the power delivered by the panels. Through transition 26, the marking of place 16 representing the panel is determined by Simulink. This means that the number of tokens in place 16 corresponds to the power delivered by the panels. The transfer of real measurements into the Petri net requires that those values are discretized and quantified into tokens. For instance, 1 token in place 16 means that the panels are delivering 1Kw power. The same reasoning is applied to velocity which means that and 1 token in place 15 corresponds to a specific value cruise velocity for the vehicle. This calculation assumes that speed varies linearly with power. This linearity can actually be verified for low velocities such as the range achieve by the solar train (see [6]).

V. Supervisory Controller

The set of subsystems that form the Helianto system are controlled by a supervisor, in charge of accounting for the constraints related to the resources and operation requirements. The approach followed in the paper is that described in [4]. Two types of constraints are defined, namely involving (i) only the marking of places, and (ii) marking of places and enabled transitions. The second type can be separated into linear and generalized linear constraints.

Roughly, the first type takes the form,

$$v_x \leq u_x, \tag{1}$$

where v_x represents a transition entering place x and u_x the marking of place x.

This equation means that transition v_x is only enabled to fire when place u_x is marked. A controller that satisfies this type of constraints is easily defined by inspection, by adding arcs to the original Petri net (PN) system.

The linear constraints have the form,

$$x\, u_x + y\, u_y \leq z, \tag{2}$$

This equation ensures that the weighted sum of tokens in places u_x and u_y does not exceed the integer z. For instance if $x = y = z = 1$, the equation means that both places cannot be marked at the same time.

A constraint of this type can be written in matrix form as

$$Lu_p \leq b, \tag{3}$$

where u_p is the marking vector of the PN, L is a 1 x n integer vector and b is an integer. Following the standard development in [4] (see also [10]), the PN controller can be computed simply as

$$D_p = -LD_c$$

where D_c is the incidence matrix of the PN, L is the constraint matrix as in (3), and D_p is the incidence matrix for the additional control place. The initial marking of this place is computed as to verify constraint (3), that is

$$u' = b - Lu_0$$

where u' corresponds to the marking of the control place.

Linear generalized constraints take the following form:

$$v_x \leq b + v_y, \tag{4}$$

This equation means that transition v_x is only enabled to fire when transition v_y has fired at least b times. A controller that satisfies this type of constraints can be obtained using a method based on place invariants for generalized linear constraints.

According to this method, given the linear constraint,

$$L\, u_P + F\, q_P + C\, v_P \leq b \tag{5}$$

where u_p is the marking vector, q_p the firing vector since $t = 0$ and v_p the vector of enabled transitions. $L = F = 0$ and C is the vector obtained from the transition coefficients in (4).

and if $b - Lu_{P_0} \leq 0$

then the controller with incidence matrix and initial marking, respectively

$$D_p = -D_p^- + D_p^+ \tag{6}$$

where

$$D_p^- = max(0, LD_c + C, F) \tag{7}$$

$$D_p^+ = max(0, F - max(0, LD_c + C)) - min(0, LD_c + C) \tag{8}$$

and

$$u_{C_0} = b - Lu_{P_0} \tag{9}$$

guarantees that constraints are verified for the states resulting from the initial marking.

A first version of the supervisor accounts for a basic set of constraints, listed below. This set does not yet account for temporal constraints such as the train timetable.

1) Once the battery crosses minimum value threshold it stops discharging.
2) While the battery remains under minimum charge value, it cannot discharge.
3) The train is only allowed to begin traveling the next trunk in case the battery charge is above safe value.
4) While motor is at cruise speed mode it switches to decelerating mode when a station approaches or an obstacle is detected.
5) While motor is off it only starts when the train is set to begin the next trunk or when an obstacle, causing the train to stop, is no longer detected.
6) Cruise speed cannot exceed a certain value.

This set of constraints for the global system was defined based on (1), (2) and (4). The incident matrix used corresponds to

Restriction	Constraint	Controller place	Number of Arcs added
1	$v_{14} \leq v_{20}$	place 19	–
2	$u_9 + u_{12} \leq 1$	place 18	–
3	$v_2 \leq u_{14}$	–	2
4	$v_8 \leq u_3; v_8 \leq u_4$	–	4
5	$v_6 \leq u_1$	–	2
6	$u_{15} \leq 4$	place 17	–

Table I
SUPERVISORY CONSTRAINTS AND SOLUTIONS OBTAINED.

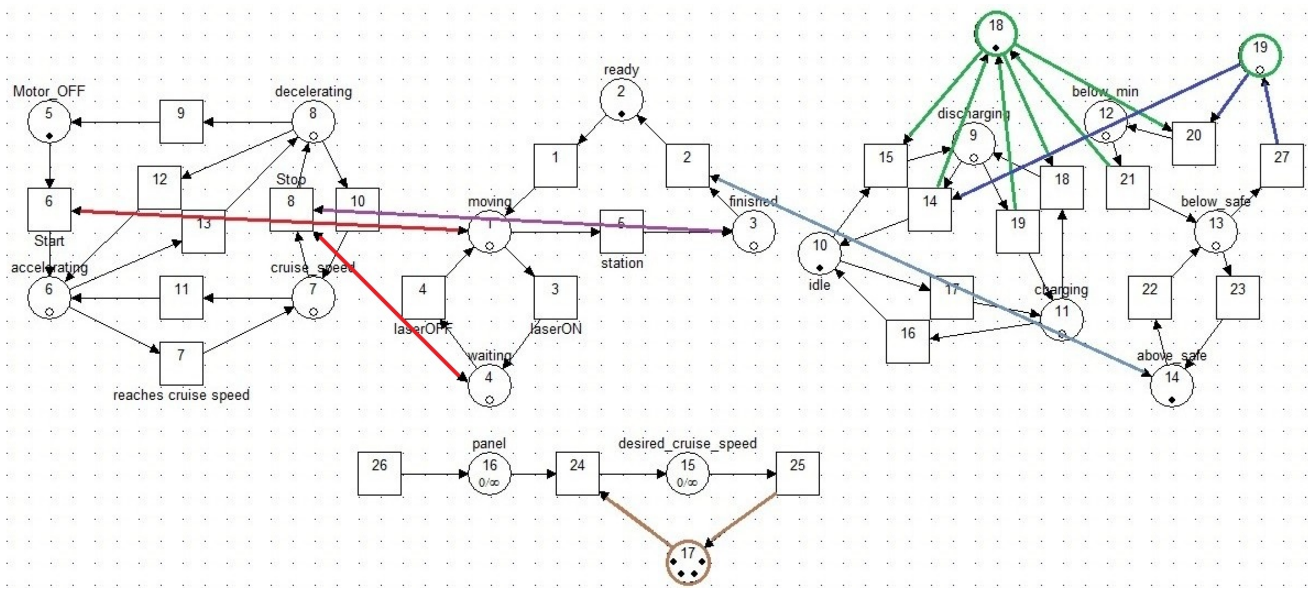

Figure 6. Petri net model of supervised system.

the global system matrix:

$$M = \begin{bmatrix} M_0 & 0 & 0 & 0 \\ 0 & M_1 & 0 & 0 \\ 0 & 0 & M_2 & 0 \\ 0 & 0 & 0 & M_3 \end{bmatrix}$$

Where M_0, M_1, M_2 and M_3 are defined in figure 5.
The corresponding supervised system is represented in figure 6 where colored arcs and places represent the controller elements added to the model. Table I summarizes the constraints as well as the controller places or arcs, on figure 6, resulting from control solutions to each constraint.

Accounting for a timetable can be done in multiple ways, e.g., (i) using a timed transition from place 7 to a new place so that the elapsed time can be counted through the marking of this new place, or (ii) simply add a new input place with the marking being defined after the events generated according to a real clock from Simulink. Each of these ways requires then an active changing of the constraint that bounds the cruise velocity, in place 15, this meaning that a minimum cruise must be defined in order to the train meet the schedule. For this task method (ii) was implemented and a new transition connected to a new place were added to the model. Since Netlab does not include timed transition elements, the transition is commanded by an external signal in Simulink that allows the firing whenever simulation time increases by one second. Once the transition fires a token is placed in the new place in order to account for the elapsed time. The same was applied to distance, and another transition and place were added to the model with the purpose of counting the covered distance. Both covered distance and elapsed time signals are transferred to Simulink so that a minimum cruise velocity is defined for the train, on a real-time basis.

VI. SIMULATION RESULTS

This section presents simulation results obtained for the model defined in the previous sections. The performance of the train is analyzed for multiple scenarios and unpredictable situations such as obstacle detection and unfavorable weather conditions. The performance of the train is evaluated based on energy consumption, time of travel and speed achieved. The power delivered by the panels varies along the day, depending directly on irradiance and on the suns' position, and therefore so does the performance of the train. The irradiance of the sun along the day corresponds to the power delivered by the sun per square meter. The panels can only absorb part of this power, though is has to be taken into account that the efficiency depends on the technology and equipment. Currently the best

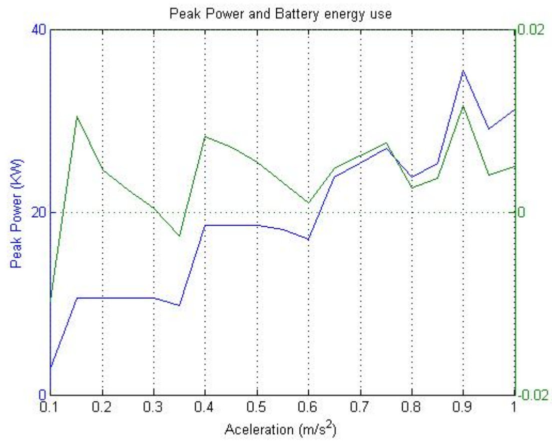

(a) Peak power and battery use vs. acceleration

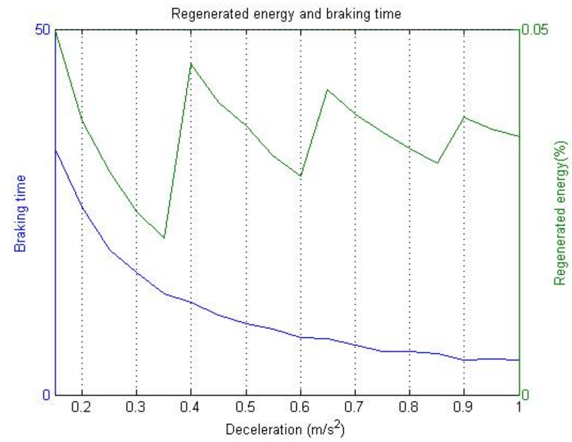

(b) Renegeration and braking time vs. deceleration

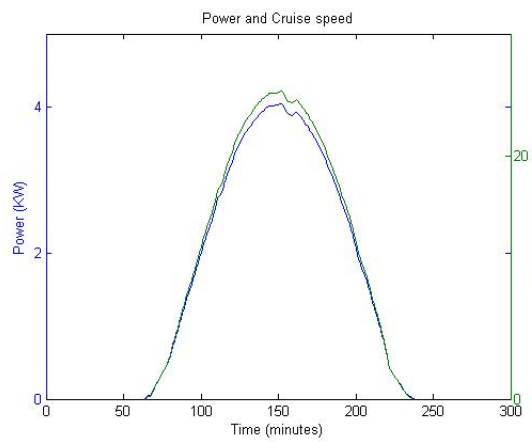

(c) Power delivered by panels and cruise velocity allowed along daytime.

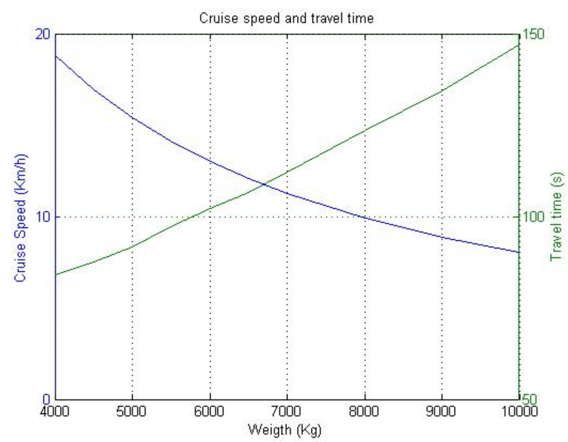

(d) Cruise speed allowed and travel time vs. weight carried by the train

Figure 7. Simulation results

achieved sunlight conversion rate (solar panel efficiency) is around 21% in commercial products [8]. This is the value assumed throughout this section.

The typical irradiance values can be obtained from a solar radiation data services website [7]. Since the main working season for the train is the summer, the values obtained correspond to an average day in June as to consider the typical summer irradiance conditions. Figure 7(c) shows the power delivered by the panels during summer, considering that the panels dimensions are 1.6x1m and that 12 panels are placed in each carriage. It is possible to see that a maximum peak of around 4 kw can be obtained between noon and 2 pm. The relation between power and speed is considered linear [6], thus the corresponding equation is obtained by applying a linear interpolation between several velocities and corresponding power demand, given by QSS. The cruise velocity curve allowed for the train, given the time of the day and considering the power delivered at that time is also represented in figure7(c). A correspondent maximum velocity of 25 km/h can be reached during peak power. Considering the purpose of the Helianto project it is considered that the minimum cruise velocity corresponds to 10 km/h. It is possible to observe that during summer months this velocity can be achieved from around 9 am to 5 pm. Until 9 am and after 5 pm the train requires the battery support in order to reach minimum cruise velocity. This requirement is assumed throughout the remaining simulations. Also, the average power delivered long the day is assumed to correspond to 3 Kw.

The acceleration phase produces a power peak demand. The train is assumed to start with fixed acceleration and a suited value must be fixed as to avoid unnecessary variations of energy demand and consequently unnecessary power peaks. A balanced acceleration value must be set so that the power peak can be sustained by the panels and battery. It must also be taken into consideration the acceleration time and passengers comfort, which means the time the train takes to reach cruise velocity should not be too high nor too low, respectively. A range of acceleration values is tested as to define a suited value for the start up of the train. A typical urban train acceleration value corresponds to 1 m/s^2 which is considered

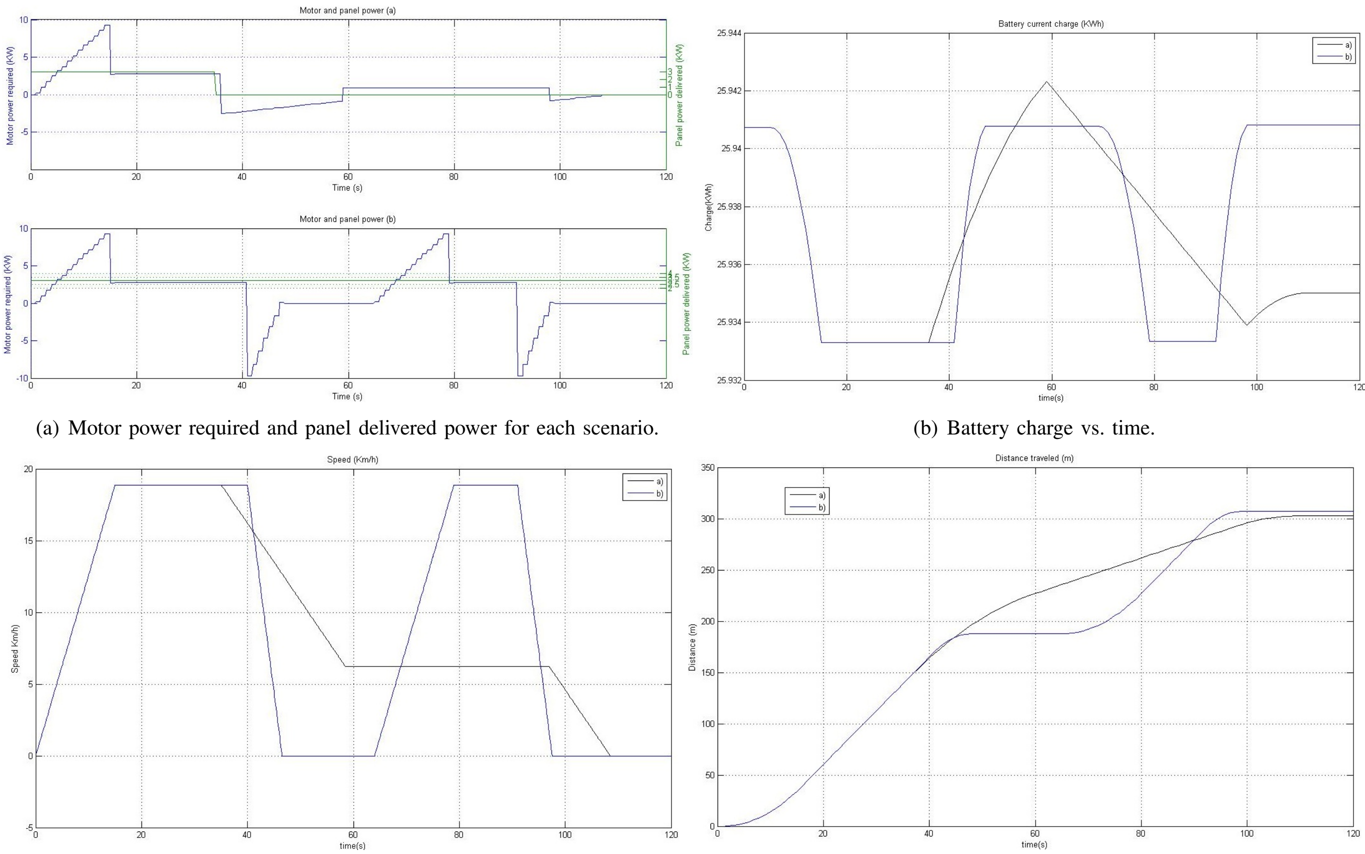

(a) Motor power required and panel delivered power for each scenario.

(b) Battery charge vs. time.

(c) Train speed vs. time.

(d) Distance traveled by the train vs. time.

Figure 8. Simulation results for two scenarios: obstacle detection (b) and power cut (a).

comfortable from the point of view of the passenger [6]. Since the solar train does not reach a typical range of speeds of an urban train, a possible range of acceleration values is considered from 0 to 1 m/s^2. This range was tested on QSS and the corresponding peak power demands and travel energy consumption are obtained and analyzed. Figure 7(a) shows the energy consumption and power peak given a range of possible acceleration values. For this situation a cruise velocity for the vehicle was fixed on 20 km/h, the road gradient and weight carried are considered null and the trunk length, braking deceleration, cruise speed and panel delivered power are constant. As expected the peak power increases with acceleration. Energy consumption is higher for the highest and lowest acceleration values. This can be explained since for the highest values the peak power is higher and therefore more energy is spent during acceleration. On the other hand for the lowest values the peak power is lower but it takes more time for the train to reach cruise speed, so the acceleration period is longer. It is intended to obtain an acceleration value that balances energy consumption, peak power and passenger comfort. This balance can be achieved by acceleration values between 0.15 and 0.35 m/s^2 where the power peak and energy consumption are lower and also it is a reasonable value from the point of view of the passengers comfort. An acceleration of 0.35 m/s^2 is assumed for all simulations described hereafter.

As the acceleration value, also the deceleration value is set to a fixed value. Deceleration is directly related to energy regeneration and therefore it must be such that regeneration is optimized. Braking time and passengers comfort must also be considered so the deceleration value should not be too low nor too high respectively. A QSS simulation was performed aiming to determine the relation between deceleration and percentage of regenerated energy and braking phase duration, when maintaining a constant route. For this simulation, a cruise velocity for the vehicle was fixed on 20 km/h and the track gradient and carried weight are considered null. The absolute deceleration value was linearly increased in order to observe the regenerated energy and braking time evolution. Figure 7(b) shows the energy regeneration and travel time given a range of possible deceleration values. As predicted, braking phase duration decreases for higher deceleration values, this happens because the higher the deceleration value, the later the train brakes in order to stop at the station.

Regeneration increases with deceleration. However it is also necessary to consider passenger comfort, and therefore deceleration cannot be too high. A reasonable value for deceleration can be found between 0.6 and 0.8 m/s^2. A deceleration of -0.8 m/s^2 is assumed for all simulations described hereafter.

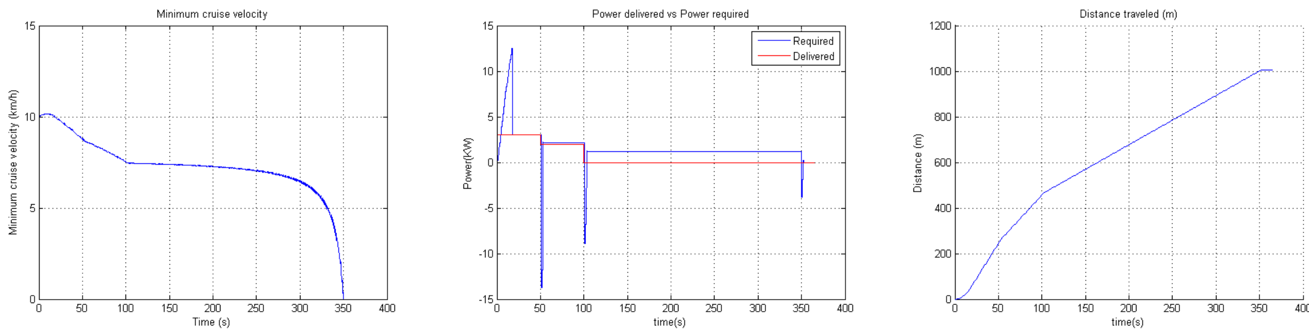

(a) Minimum velocity required to reach the target within schedule.

(b) Battery charge vs. time.

(c) Distance traveled by the train vs. time.

Figure 9. Simulation results timed mission.

The weight carried by the train influences the power demand and consequently the velocity of the train. Figure 7(d) shows travel time and cruise velocity given the weight carried by the train, considering the same amount of power available. It is possible to see that the higher the weight the lower the cruise velocity reached by the train. Consequently the travel time increases with weight. For a weight exceeding 8 tonnes it is possible to see that the cruise velocity is lower than the minimum value of 10 km/h. This means that for this weight the train requires the use of the battery in order to achieve minimum cruise velocity.

The results of two simulations on different scenarios are presented in figure 8, namely (a) a power loss that prevents the panels from delivering power (for instance, cloudy weather), and (b) an obstacle is detected on the track. The train is intended to travel 1 Km and the power delivered by the panels is 3 Kw. The battery initial charge is set to 7 kwh.

Figure 8(c) shows the velocity plot for each simulation. For the obstacle scenario (b) the train reaches cruise speed around time unit 15. On time unit 40, when the obstacle is detected, the train brakes and stops. The obstacle detection is lost at time 65, when the train accelerates and reaches cruise speed again. Once it reaches final destination it decelerates again until it stops.

For this scenario it is also possible to see, in figure 8(b), that the battery discharges only during acceleration and charges during deceleration when regeneration occurs. During cruise speed the battery keeps its charge since the power delivered by the panels is able to support speed above minimum.

For scenario (a) once the power loss is detected, the train decelerates until it reaches minimum speed. this speed is mandatory since it guarantees the train reaches the destination within the time goal. This speed is supported exclusively by the battery, since the panels are delivering no power. Figure 8(b) shows that during this time the battery is discharging as expected, until the train approaches the station.

Figure 8(a) represents the power required by the motor and the power delivered by the panels. It is possible to see in figure 8(b) that whenever the demand is larger than the power delivered, the battery discharges. This verifies for the acceleration phase and also during the power cut, in order to support the minimum speed.

Figure 8(d) represents the distance traveled by the train during simulation. By comparing these graphics with the speed profile shown in 8(c) it is possible to see that the model is consistent.

Following the discussion in section V, accounting for a time schedule was implemented by feeding the Petri net model with a timing signal from the external environment. A simulation was performed where the train is required to travel 1 Km within a maximum time of 360 s. The results are presented in figure 9.

Figure 9 (a) presents the minimum velocity required in order to reach the target within the maximum time given. A higher velocity is allowed as long as the panels are able to sustain it. For this case through figure 9 (b) it is possible to see that until time unit 100, the panels are able to sustain a higher velocity, which causes the minimum velocity value to decrease as time passes. From that time instant forward the panels stop delivering power, which causes the train to assume the value of minimum velocity, in order to reach the target in time. The train travels at this velocity until it stops at the target, within the defined schedule and therefore accomplishing the proposed time goal.

VII. Conclusions

This paper describes a simulation tool to assess the viability of the Helianto solar train project.

The whole infrastructure was modeled as a discrete events system (DES), represented by Petri nets, and a supervisory controller was designed for the whole system. The development of the simulation model addressed two main issues: the vehicle dynamics and the DES modeling. Two key toolboxes were used for these purposes, respectively, QSS and Netlab. The performance of the train is analyzed for multiple scenarios and evaluated based on energy consumption,travel time and speed achieved.

The influence of variables such as weight and road gradient is studied, and conclusions are drawn for the maximum values allowed for these variables. Suitable constant acceleration and deceleration (when braking) are also studied aiming at minimizing the energy consumption and increasing regeneration.

Simulations are performed on two different scenarios. The first scenario refers to a situation where a obstacle is detected on the track and the second refers to a power cut during travel. Solutions to both situations are presented as also results validating the model. Temporal constraints such as the ones introduced by time schedules are also accounted. The results were consistent showing that the velocity achieved by the vehicle allowed the vehicle motion to be energetically sustained by the panels alone, resorting to battery only during acceleration phase, where a power peak demand occurs, or when a power failure occurs in order to sustain minimum velocity. The train reaches the station within the required time, complying with the schedule. Additionally, once an obstacle is detected, the train stops, resuming travel once detection is lost.

The results obtained show consistency in the sense that the train behaves as realistically expected and the energy consumption was effectively managed. It also proved to be a very practical tool that allows the simulation of multiple types of vehicles, multiple track features, different energy sources, as well as, different performance purposes, for the vehicle.

ACKNOWLEDGMENTS

This work was partially supported by FCT project PEst-OE/EEI/LA0009/2011.

REFERENCES

[1] M. Godoy Simaes, N. N. Franceschetti and J. C. Adamowski. Drive System Control and Energy Management of a Solar Powered Electric Vehicle. University of Sao Paulo, Sao Paulo, Brazil, 1998

[2] Jinrui N, Fengchun S and Qinglian R. A Study of Energy management System of Electric Vehicles. School of mechanical and vehicular engineering, Beijing Institute of Technology, Beijing, China,2006.

[3] L. Warrington and J. A. Jones. Representing Complex Systems within Discrete Event Simulation for Reliability Assessment. Coventry International Manufacturing Centre, Department of Engineering, University of Warwick, Coventry, United Kingdom, 2003.

[4] J.Moody, K.Yamalidou, P.Antsaklis and M.Lemmon. Feedback control of Petri Nets based on place invariants. Department of Electrical Engineering, University of Notre Dame, Notre Dame, 1994.

[5] R. Davidrajuh. Developing a New Petri net Tool for Simulation of Discrete Event Systems. University of Stavanger, Stavanger, Norway,2008.

[6] J.M.C.S.André. *Transporte Interurbano em Portugal*.vol 2. Lisbon, IST Press, 2006.

[7] http://www.soda-is.com. Accessed January 2012.

[8] The independent, ”World's most efficient solar panel”, http://www.independent.co.uk/environment/worlds-most-efficient-solar-cells-ready-for-use-in-the-uk-2200508.html. Accessed April 2012

[9] Christos G Cassandras, Stephane Lafortune, ”Introduction to Discrete Event Systems”, Springer, 2008

[10] Stjepan Bogdan, Frank Lewis, Zdenki Kovacic, José Meireles Jr, ”Manufacturing Systems Control Design: A Matrix Based Approach”, Springer, 2006

[11] Institute of Automatic Control, RWTH Aachen University, ”Petri Net Toolbox: Netlab”, http://www.irt.rwth-aachen.de/en/fuer-studierende/downloads/petri-net-tool-netlab/. 2008

[12] Swiss Federal Institute of Technology Zurich, ”QSS-Toolbox”, http://www.idsc.ethz.ch/Downloads/qss. 2008